Post-buckling analysis of Timoshenko beams made of functionally graded material under thermal loading

Turgut Kocatürk* and Şeref Doğuşcan Akbaş[a]

*Department of Civil Engineering, Yildiz Technical University, Davutpasa Campus,
34210 Esenler-İstanbul, Turkey*

Abstract. This paper focuses on post-buckling analysis of functionally graded Timoshenko beam subjected to thermal loading by using the total Lagrangian Timoshenko beam element approximation. Material properties of the beam change in the thickness direction according to a power-law function. The beam is clamped at both ends. The considered highly non-linear problem is solved by using incremental displacement-based finite element method in conjunction with Newton-Raphson iteration method. As far as the authors know, there is no study on the post-buckling analysis of functionally graded Timoshenko beams under thermal loading considering full geometric non-linearity investigated by using finite element method. The convergence studies are made and the obtained results are compared with the published results. In the study, with the effects of material gradient property and thermal load, the relationships between deflections, end constraint forces, thermal buckling configuration and stress distributions through the thickness of the beams are illustrated in detail in post-buckling case.

Keywords: functionally graded materials; geometrical non-linearity; post-buckling analysis; total lagrangian finite element model; Timoshenko beam; temperature loading

1. Introduction

Functionally graded materials (FGMs) are a new generation of composites where the volume fraction of the FGM constituents vary gradually, giving a non-uniform microstructure with continuously graded macro properties such as elasticity modulus, density, heat conductivity, etc.. Typically, in an FGM, one face of a structural component is ceramic that can resist severe thermal loading and the other face is metal which has excellent structural strength. FGMs consisting of heat-resisting ceramic and fracture-resisting metal can improve the properties of thermal barrier systems because cracking and delamination, which are often observed in conventional layered composites, are reduced by proper smooth transition of material properties. FGMs have many practical applications, such as reactor vessels, biomedical sectors, aircrafts, space vehicles, defense industries and other engineering structures. Especially, as aerospace vehicles, nuclear power plants, thermal power plants etc. are subject to thermal loadings, FGMs have found extensive applications in these applications. With the increased use of FGMs, understanding the mechanical behavior of FG

---

*Corresponding author, Professor, E-mail: kocaturk@yildiz.edu.tr
[a]Ph.D. Student

structures is very important. In recent years, much more attention has been given to the thermal buckling of FG beam structures. Thermal buckling of thick, moderately thick and thin cross-ply laminated beams subjected to uniform temperature distribution are analyzed by Khdeir (2001). Thermoelastic equilibrium equations for a functionally graded beam are solved in closed-form to obtain the axial stress distribution by Sankar and Tzeng (2002). Thermal buckling load of a curved beam made of functionally graded material with doubly symmetric cross section is investigated by Rastgo *et al*. (2005). Ching and Yen (2005) studied 2D functionally graded solids, which is subjected to either mechanical or thermal loads by using the meshless local Petrov-Galerkin method. Three – dimensional surface cracking of a graded coating bonded to a homogeneous substrate is studied by Inan *et al*. (2005). Librescua *et al*. (2005) investigated the thermoelastic modelling and behaviour of thin-walled beams made of functionally graded materials. Ching and Yen (2005) studied Transient thermoelastic deformations of functionally graded (FG) beams by using the meshless local Petrov-Galerkin method. Li *et al*. (2006) investigated thermal post-buckling of Functionally Graded clamped-clamped Timoshenko beams subjected to transversely non-uniform temperature. Buckling and vibration behaviour of a functionally graded sandwich beam having constrained viscoelastic layer is studied in thermal environment by using finite element formulation by Bhangale and Ganesan (2006). Nirmula *et al*. (2006) derived analytical expressions for the thermo-elastic stresses in a three-layered composite beam system whose middle layer is a functionally graded material. Three-dimensional thermal buckling and postbuckling analyses of functionally graded materials subjected to uniform or non-uniform temperature rise are examined by using finite element method by Na and Kim (2006). Two-dimensional thermoelasticity analysis of functionally graded thick beams is presented using the state space method coupled with the technique of differential quadrature by Lu *et al*. (2006). Thermoelastic stress field in a functionally graded curved beam, where the elastic stiffness varies in the radial direction, is considered by Mohammadia and Drydena (2008). The problem of thermo-elastic stress analysis in multi-layered nonhomogeneous beams is considered by Carpinteri and Paggi (2008). Rahimi and Davoodinik (2008) studied thermal behaviour analysis of the functionally graded Timoshenko beam. A third-order zigzag theory based finite element model in conjunction with the modified rule of mixtures and Wakashima-Tsukamoto model for estimating effective modulus of elasticity and coefficient of thermal expansion, respectively, is presented for layered functionally graded beams under thermal loading by Kapuria *et al*. (2008). Based on Kirchhoff's assumption of straight normal line of beams and considering the effects of the axial elongation, the initial curvature and the stretching-bending coupling on the arch deformation, geometrically nonlinear governing equations of functionally graded arch subjected to mechanical and thermal loads are derived by Song and Li (2008). The free and forced vibration of a laminated functionally graded beam of variable thickness under thermally induced initial stresses is studied within the framework of Timoshenko beam theory by Xiang and Yang (2008). Free vibration analysis of thermal postbuckled functionally graded beams with surface-bonded piezoelectric layers subject to both temperature rise and voltage is studied by Li *et al*. (2009). The postbuckling response of beams made of functionally graded materials (FGMs) containing an open edge crack is studied based on Timoshenko beam theory and von Kármán nonlinear kinematics by Ke *et al*. (2009). Thermo-mechanical vibration analysis of functionally graded beams and functionally graded sandwich beams are presented by Pradhan and Murmu (2009). Lim *et al*. (2009) investigated temperature-dependent in-plane vibration of functionally graded (FGM) circular arches based on the two-dimensional theory of elasticity. Malekzadeh *et al*. (2010) presented a first known formulation for the out-of-plane free vibration analysis of

functionally graded circular curved beams in thermal environment. Buckling of beams made of functionally graded material under various types of thermal loading is studied based on the Euler–Bernoulli beam theory by Kiani and Eslami (2010). Alibeigloo (2010) investigated analytical solution for functionally graded beams integrated with piezoelectric actuator and sensor under an applied electric field and thermo-mechanical load. Thermal post-buckling behaviour of uniform slender FG beams is investigated independently using the classical Rayleigh-Ritz (RR) formulation and the versatile finite element analysis based on the von-Karman strain-displacement relations by Anandrao *et al*. (2010). Free vibration analysis of initially stressed thick simply supported functionally graded curved panel resting on two-parameter elastic foundation (Pasternak model), subjected in thermal environment is studied using the three-dimensional elasticity formulation by Farid *et al*. (2010). Kocaturk *et al*. (2011) investigated the full geometrically non-linear static analysis of a cantilever Timoshenko beam composed of functionally graded material under a non-follower transversal uniformly distributed load. Akbas (2011) studied termal post – buckling of functionally graded beams. Akbas and Kocaturk (2011) studied post- buckling analysis of an axially functionally graded simple beam within Timoshenko beam theory under temperature rising. Also, Akbas and Kocaturk (2011), Kocaturk and Akbas (2011) investigated post buckling analysis of beams under uniform and non-uniform temperature rising respectively considering full geometric non-linearity.

   As far as the authors know, there is no study on the post-buckling analysis of FG Timoshenko beams under thermal loading considering full geometric non-linearity investigated by using finite element method: In the present study, the post buckling analysis of FG clamped-clamped Timoshenko beams under thermal loading is considered by using the total Lagrangian finite element method by taking into account full geometric nonlinearity.

   The development of the formulations of general solution procedure of nonlinear problems follows the general outline of the derivation given by Zienkiewichz and Taylor (2000). The related formulations of post-buckling analysis of FG Timoshenko beam subjected to thermal loading are obtained by using the total Lagrangian finite element model of FG Timoshenko beam. Convergence studies are performed for various numbers of elements. In deriving the formulations for post buckling analysis of FG Timoshenko beams under thermal loading, the total Lagrangian Timoshenko beam element formulations for homogeneous material given by Felippa (2011)] are used. There is no restriction on the magnitudes of deflections and rotations in contradistinction to von-Karman strain displacement relations of the beam. With the effects of material gradient property on the post-buckling, the relationships between deflections, end rotational angles, end constraint forces, thermal buckling configuration, stress distributions through the thickness of the beams and temperature rising are illustrated in detail in post-buckling case.

2. Theory and formulations

   The clamped-clamped beam configurations, made of functionally graded elastic material, with co-ordinate system $O(XYZ)$ are shown in Fig. 1.

   In this study, it is assumed that the FG beam is made of ceramic and metal, and the effective material properties of the FG beam, P, i.e., Young's modulus E, coefficient of thermal expansion α_X, coefficient of thermal conductivity K, temperature rise T, Poisson's ratio υ and shear modulus G vary continuously in the thickness direction (Y axis) according to a power-law function (1990) as follows
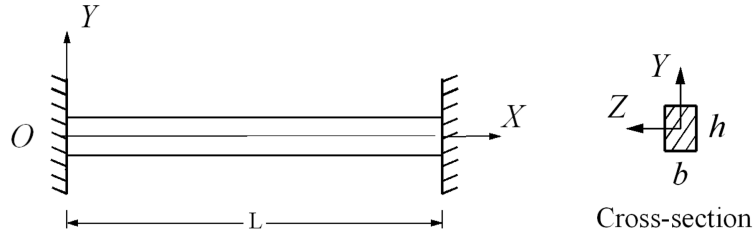
Fig. 1 Clamped-clamped beam and cross-section

$$P(Y) = (P_T - P_B)\left(\frac{Y}{h} + \frac{1}{2}\right)^n + P_B \tag{1}$$

where P_T and P_B are the material properties of the top and the bottom surfaces of the beam. It is clear from Eq. (1) that when $Y = -h/2$, $P = P_B$, and when $Y = h/2$, $P = P_T$. where n is the non-negative power-law exponent which dictates the material variation profile through the thickness of the beam.

The considered problem is a nonlinear one. Even linear problems may not admit exact solutions due to geometric and material complexities, but it is relatively easy to obtain approximate solutions using numerical methods (Reddy 2004). For the solution of the total Lagrangian formulations of TL plane beam problem, small-step incremental approaches from known solutions are used. In this study, the TL Timoshenko beam element is used and the related formulations are developed by using the formulations given by Kocatürk *et al.* (2011) which was developed for FG beam by using the formulations given by Felippa (2011) for isotropic and homogeneous beam material. Interested reader can find the related formulations in Kocatürk *et al.* (2011) and Felippa (2011).

The second Piola-Kirchhoff stresses with a temperature rise can be expressed by inclusion of the temperature term as follows

$$\mathbf{s} = \begin{bmatrix} s_{XX} \\ s_{XY} \end{bmatrix} = \begin{bmatrix} s_1 \\ s_2 \end{bmatrix} = \begin{bmatrix} s_1^0 + E(Y)(e_1 - \alpha_X(Y)T(Y)) \\ s_2^0 + G(Y)e_2 \end{bmatrix} = \begin{bmatrix} s_1^0 \\ s_2^0 \end{bmatrix} + \begin{bmatrix} E(Y) & 0 \\ 0 & G(Y) \end{bmatrix}\begin{bmatrix} e_1 - \alpha_X(Y)T(Y) \\ e_2 \end{bmatrix} \tag{2}$$

where s_1^0, s_2^0 are initial stresses, E is the modulus of elasticity and G is the shear modulus, α_X is coefficient of thermal expansion in the X direction and T is the temperature rise and their dependence on Y coordinate are given by Eq. (1). The temperature rise $T = T(Y)$ is governed by heat transfer equation of

$$-\frac{d}{dY}\left[K(Y)\frac{dT(Y)}{dY}\right] = 0 \tag{3}$$

By integrating Eq. (3) using boundary conditions $T(h/2) = T_T$ and $T(-h/2) = T_B$, the following expression can be obtained

$$T(Y) = T_B + (T_T - T_B)\int_{-h/2}^{y}\frac{1}{K(Y)}dY \Big/ \int_{-h/2}^{h/2}\frac{1}{K(Y)}dY \tag{4}$$

where K is the coefficient of thermal conductivity and dependence on Y coordinate are given by Eq. (1).

Using constitutive Eq. (2), axial force N, shear force V and bending moment M can be obtained as

$$N = \int_A s_1 dA = \int_A [s_1^0 + E(Y)(e - Y\kappa - \alpha_X(Y)T(Y))]dA = N^0 + A_{xx}e - B_{xx}\kappa - N_T \tag{5}$$

$$V = \int_A s_2 dA = \int_A [s_2^0 + G(Y)e_2]dA = V^0 + A_{xx}\gamma \tag{6}$$

$$M = \int_A -Ys_1 dA = \int_A -Y[s_1^0 + E(Y)(e - Y\kappa - \alpha_X(Y)T(Y))]dA \tag{7}$$

$$M = M^0 - B_{xx}e + D_{xx}\kappa - M_T \tag{8}$$

where e, γ and κ are axial strain, shear strain and curvature of the beam, respectively. The details of these expressions can be found in Kocatürk *et al*. (2011) and Felippa (2011).

$$N^0 = \int_{A_0} s_1^0 dA, \quad V^0 = \int_{A_0} s_2^0 dA, \quad M^0 = \int_{A_0} -Ys_1^0 dA \tag{9}$$

$$(A_{xx}, B_{xx}, D_{xx}) = \int_A E(Y)(1, Y, Y^2)dA \tag{10}$$

$$A_{xz} = \int_A G(Y)dA \tag{11}$$

$$(N_T, M_T) = \int_A E(Y)\alpha(Y)T(Y)(1, Y)dA \tag{12}$$

where A_{xx}, B_{xx}, D_{xx} and A_{xz}, are the extensional, coupling, bending transverse shear rigidities, respectively. N_T and M_T are the thermal axial force and the bending moment, respectively.

For the solution of the total Lagrangian formulations of TL Timoshenko beam element, small-step incremental approaches from known solutions with Newton-Raphson iteration method are used in which the solution for $n + 1$th load increment and ith iteration is obtained in the following form

$$d\mathbf{u}_n^i = (\mathbf{K}_T^i)_S^{-1}(\mathbf{R}_{n+1}^i)_S \tag{13}$$

where $(\mathbf{K}_T^i)_S$ is the system stiffness matrix corresponding to a tangent direction at the ith iteration, $d\mathbf{u}_n^i$ is the solution increment vector at the ith iteration and $n + 1$th load increment, $(\mathbf{R}_{n+1}^i)_S$ is the system residual vector at the ith iteration and $n + 1$th load increment. This iteration procedure is continued until the difference between two successive solution vectors is less than a selected tolerance criterion in Euclidean norm given by

$$\sqrt{\frac{[(d\mathbf{u}_n^{i+1} - d\mathbf{u}_n^i)^T(d\mathbf{u}_n^{i+1} - d\mathbf{u}_n^i)]^2}{[(d\mathbf{u}_n^{i+1})^T(d\mathbf{u}_n^{i+1})]^2}} \leq \zeta_{tol} \tag{14}$$

A series of successive approximations gives

$$\mathbf{u}_{n+1}^{i+1} = \mathbf{u}_{n+1}^{i} + d\mathbf{u}_{n+1}^{i} = \mathbf{u}_n + \Delta\mathbf{u}_n^i \tag{15}$$

where

$$\Delta\mathbf{u}_n^i = \sum_{k=1}^{i} d\mathbf{u}_n^k \tag{16}$$

The residual vector $\mathbf{R}_{n+1}^i$ for a finite element is as follows

$$\mathbf{R}_{n+1}^i = \mathbf{f} - \mathbf{p} \tag{17}$$

where $\mathbf{f}$ is the vector of external forces and $\mathbf{p}$ is the vector of internal forces given by Felippa (2011).

The element tangent stiffness matrix for the total Lagrangian Timoshenko plane beam element is as follows which is given by Felippa (2011)

$$\mathbf{K}_T = \mathbf{K}_M + \mathbf{K}_G \tag{18}$$

where $\mathbf{K}_G$ is the geometric stiffness matrix, and $\mathbf{K}_M$ is the material stiffness matrix given as follows by Felippa (2011)

$$\mathbf{K}_M = \int_{L_0} \mathbf{B}_m^T \mathbf{S} \mathbf{B}_m dX \tag{19}$$

The interested reader can find the explicit forms of the expressions in Eq. (19) in Kocatürk *et al.* (2011) and Felippa (2011). After integration of Eq. (19), K_M can be expressed as follows

$$\mathbf{K}_M = \mathbf{K}_M^a + \mathbf{K}_M^c + \mathbf{K}_M^b + \mathbf{K}_M^s \tag{20}$$

where $\mathbf{K}_M^a$ is the axial stiffness matrix, $\mathbf{K}_M^b$ is the bending stiffness matrix, $\mathbf{K}_M^s$ is the shearing stiffness matrix and explicit forms of these expressions are given by Felippa (2011). As defined before, A_{xx}, B_{xx}, D_{xx} and A_{xz} are the extensional, coupling, bending and transverse shear rigidities, respectively. A_{xx} appear in the matrix $\mathbf{K}_M^a$, D_{xx} appear in the matrix $\mathbf{K}_M^b$, A_{xz} appear in the matrix $\mathbf{K}_M^s$. These A_{xx}, D_{xx} and A_{xz} quantities are calculated for FG beam by Kocatürk *et al.* (2011) and replaced in the related stiffness matrixes. $\mathbf{K}_M^c$ is the coupling stiffness matrix which arose for FG material and obtained by Kocatürk *et al.* (2011).

The geometric stiffness matrix K_G and the internal nodal force vector $\mathbf{p}$ remains the same as given by Felippa (2011).

After obtaining the displacements of nodes, the second Piola-Kirchhoff stress tensor components S_{xx}, S_{xy}, S_{yy} can be obtained by using Eq. (2). The relation between the Cauchy stress tensor components $\sigma_{xx}, \sigma_{xy}, \sigma_{yy}$ and the second Piola-Kirchhoff stress tensor components S_{xx}, S_{xy}, S_{yy} is given in Kocatürk *et al.* (2011) and Felippa (2011).

The beams considered in numerical examples are elastic, with undeformed length L, rectangular cross-section of width b and thickness h (see Fig. 1). The dimensionless quantities can be expressed as

$$\xi = \frac{X}{L}, \quad \eta = \frac{Y}{L}, \quad U = \frac{u_x}{L}, \quad V = \frac{u_y}{L}$$

$$E_r = \frac{E_T}{E_B}, \quad \alpha_r = \frac{\alpha_T}{\alpha_B}, \quad T_r = \frac{T_T}{T_B}, \quad \lambda = \delta^2 \alpha_B T_B$$

$$R_H = \frac{r_H L^2}{D_{XX}}, \quad R_V = \frac{r_V L^2}{D_{XX}}, \quad R_T = \frac{N_T L^2}{D_{XX}}$$

$$m = \frac{mL}{D_{XX}}, \quad m_T = \frac{M_T L}{D_{XX}}, \quad \Delta = \frac{S-L}{L}, \quad \delta = \frac{L}{h}$$

$$\overline{\sigma}_{xx} = \frac{\sigma_{xx}}{E_B T_B \alpha_{xB}}, \quad \overline{\sigma}_{yy} = \frac{\sigma_{yy}}{E_B T_B \alpha_{xB}}, \quad \overline{\sigma}_{xy} = \frac{\sigma_{xy}}{E_B T_B \alpha_{xB}} \tag{21}$$

where T_r is the ratio of temperature rise of top and bottom surfaces of the beam, E_r is the ratio of Young's modulus of top and bottom surfaces of the beam, α_r is the ratio of coefficient of thermal expansion of top and bottom surfaces of the beam, λ is dimensionless thermal load, R_H is dimensionless constraint force in the horizontal direction, R_V is dimensionless constraint force in the vertical direction, R_T is dimensionless thermal axial force, m is dimensionless constraint moment, m_T is dimensionless thermal bending moment, Δ is the total dimensionless axial extension, S is the length of the beam after deformation, δ is the ratio of L/h (lenght/height), $\overline{\sigma}_{xx}, \overline{\sigma}_{yy}$ are dimensionless Cauchy normal stresses and $\overline{\sigma}_{xy}$ is dimensionless Cauchy shear stress.

3. Numerical results

In the numerical examples, the post-buckling deflections as well as the Cauchy maximum and minimum principal normal stresses, thermal axial force, thermal bending, critical buckling temperature, axial extension, end constraint moment are calculated and presented in figures for different material composition and various thermal loads. To this end, by use of usual assembly process, the system tangent stiffness matrix and the system residual vector are obtained by using the element stiffness matrixes and element residual vectors for the total Lagrangian Timoshenko plane beam element. After that, the solution process outlined in the previous section is used for obtaining

Table 1 Convergence analysis for the dimensionless central deflections $V(0.5)$ of the beam number of finite elements m for material power law index $n = 3$, $T_r = 4$ and $L/h = 6$

The dimensionless central deflections $V(0.5)$ of the beam	
m	$\lambda = 4$
6	0.2022
10	0.2053
20	0.2059
30	0.2060
40	0.2060
50	0.2060

the related solutions for the total Lagrangian finite element model of Timoshenko plane beam element. The beam considered in numerical examples is made of Aluminum (Al; $E = 70$ GPa, $v = 0.31$, $K = 204$ W/(m.K), $\alpha = 23 \times 10^{-6}$ K^{-1}) and Zirconia (ceramic) (ZrO$_2$; $E = 151$ GPa, $v = 0.2882$, $K = 2.09$ W/(m.K), $\alpha = 10 \times 10^{-6}$ K^{-1}). When the power index $n = 0$, the beam material is reduced to full ceramic (homogeneous ceramic). The bottom surface of the FG beam is Aluminum, whereas the top surface of the FG beam is Zirconia (ceramic). Convergence and comparison studies are also performed. In the geometrically non-linear case, the Cauchy stresses (true stresses) can be obtained after obtaining the second Piola-Kirchhoff stresses by using Eq. (8) by using the relation between the Cauchy and the second Piola-Kirchhoff stresses tensor components is given in Kocatürk *et al*. (2011) and Felippa (2011).

In Table 1, the dimensionless central deflections $V(0.5)$ for dimensionless thermal load parameter $\lambda = 4$ are calculated for various numbers of finite elements m for the material power law index $n = 3$, ratio of temperature rise of top and bottom surfaces of the beam $T_r = 4$ and $L/h = 6$. It is seen from Table 1 that, when the number of finite elements is $m = 50$, the considered displacements converge perfectly. Therefore, in the numerical calculations, the number of finite elements is taken as $m = 50$.

In order to establish the accuracy of the present formulation and the computer program developed by the authors, the results obtained from the present study are compared with the available results in the literature. For this purpose, the dimensionless thermal axial forces R_T are calculated for various material power law index n for $L/h = 15$, $\lambda = 2$ and $T_r = 1, 2, 3$ for clamped-clamped beam and compared with those of Li *et al*. (2006). It is clearly seen that the curves of Fig. 2 of the present study are very close to those of Fig. 3 of Li *et al*. (2006).

To further verify the present results, the dimensionless specified deflections $V(0.5)$ are calculated for various material power law index n for $L/h = 15$, $T_r = 15$ and dimensionless thermal load parameter $\lambda = 2, 3, 5$ for clamped-clamped beam and compared with those of Li *et al*. (2006). Comparisons of Fig. 3 with Fig. 7 of Li *et al*. (2006) show that the curves of the present study are very close to those of Li *et al*. (2006).

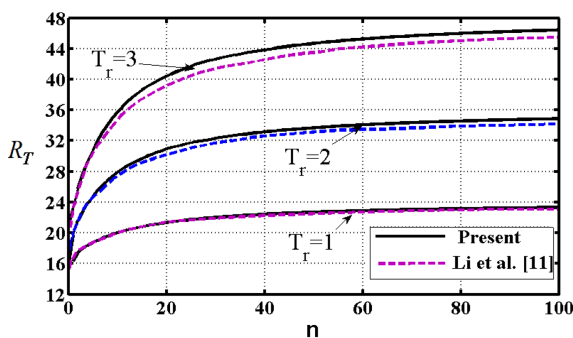The dimensionless thermal bending moments M_T are calculated for various material power law

Fig. 2 The dimensionless thermal axial force R_T versus material power law index n for $L/h = 15$, $\lambda = 2$ and $T_r = 1, 2, 3$ for clamped-clamped beam
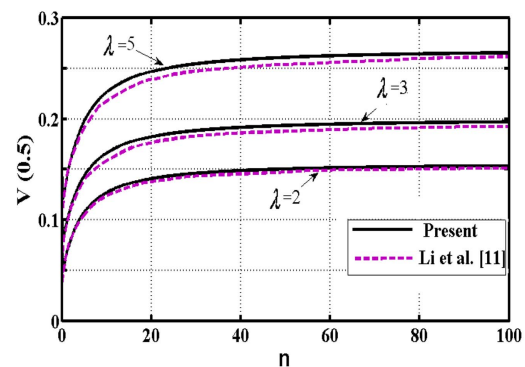
Fig. 3 The dimensionless specified deflections $V(0.5)$ versus the material power law index n for $L/h = 15$, $T_r = 15$ and dimensionless thermal load parameter $\lambda = 2, 3, 5$ for clamped-clamped beam
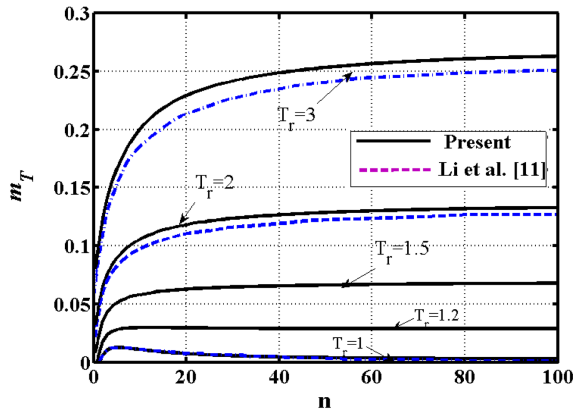
Fig. 4 The dimensionless thermal bending M_T with various the material power law index n for $L/h = 15$, $\lambda = 2$ and the material power law index $T_r = 1$, 1.2, 1.5, 2, 3 at clamped-clamped beam
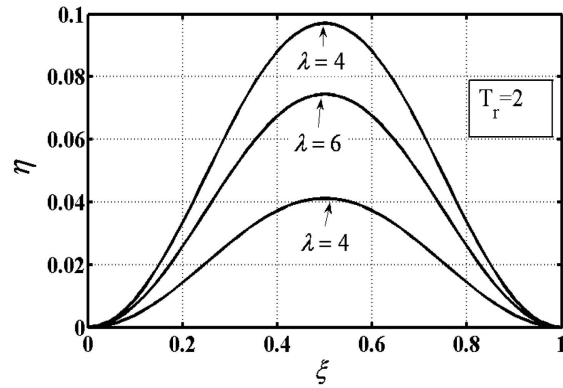

Fig. 5 Thermal buckling configuration of the beam for $T_r = 2$, $L/h = 15$, $n = 3$, $\lambda = 4$, 6, 8
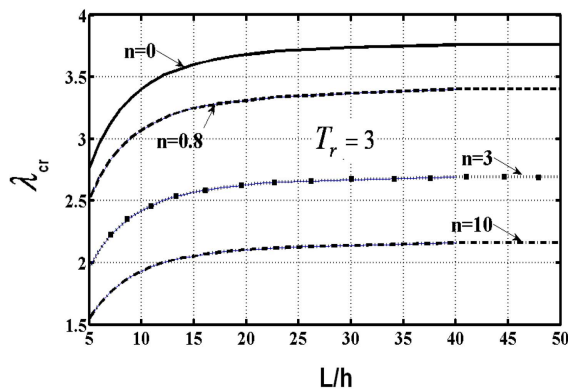

Fig. 6 Dimensionless critical buckling temperature versus slenderness ratio for various material power law index n for $T_r = 3$
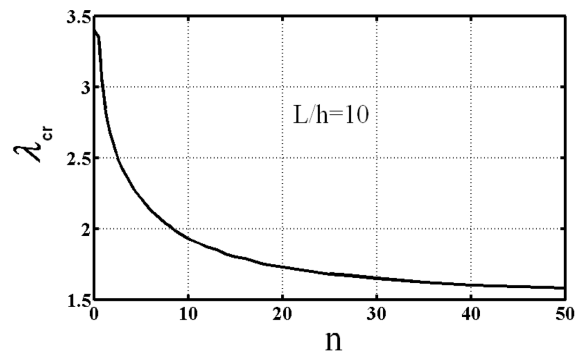

Fig. 7 Dimensionless critical buckling temperature versus the material power law index n for $L/h = 10$ and $T_r = 3$

index n for $L/h = 15$, $T_r = 1, 1.2, 1.5, 2, 3$ and dimensionless thermal load parameter $\lambda = 2$ for clamped-clamped beam and compared with those of Li *et al.* (2006). Comparisons of Fig. 4 with Fig. 4 of Li *et al.* (2006) show that there is a very good harmony between the present results and those of Li *et al.* (2006).

In Fig. 5, the thermal buckled configurations of the beam are shown for $T_r = 2$, $L/h = 15$, $n = 3$, $\lambda = 4, 6, 8$.

In Fig. 6, critical buckling temperatures versus slenderness ratio are shown for various material power law index n for $T_r = 3$. It is seen from Fig. 6 that almost all of the curves have horizontal asymptotes approximately after the slenderness ratio $L/h = 30$. It is seen from Figs. 6, 7 that increase in the material power law index n causes decrease in the dimensionless critical thermal loading. The form of this decrement can be seen from Fig. 7. After the value of power law index $n = 40$, the
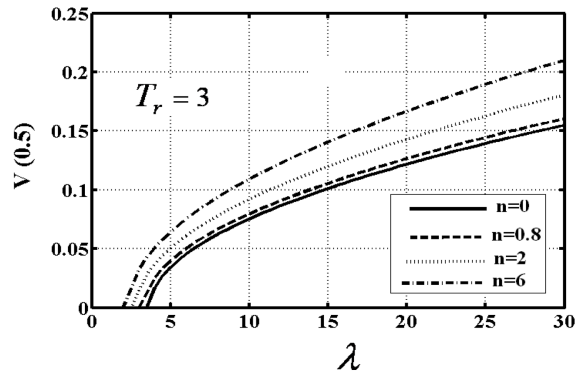
Fig. 8 The dimensionless specified deflections $V(0.5)$ versus dimensionless thermal load parameter λ for various material power law index n for $L/h = 20$
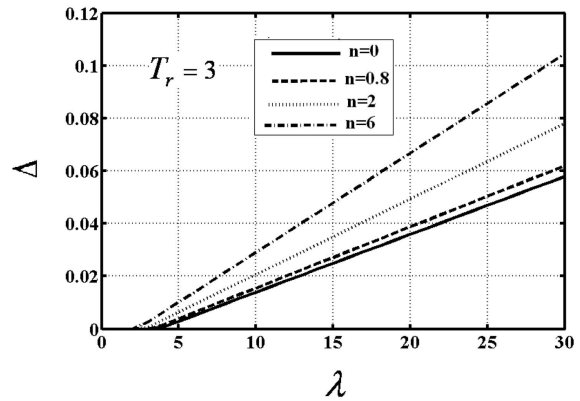
Fig. 9 The total dimensionless axial extension Δ versus various dimensionless thermal load λ for various material power law index n for $L/h = 20$
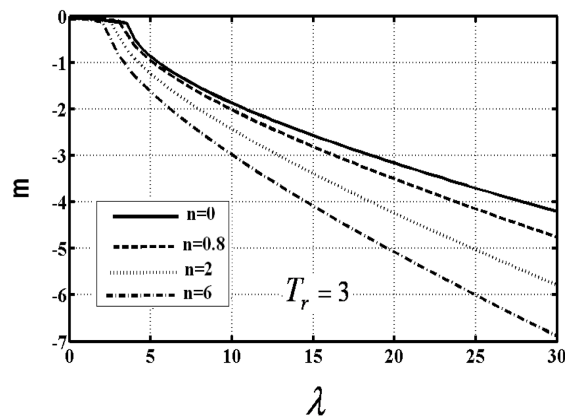

Fig. 10 The dimensionless end constraint moment m versus dimensionless thermal load parameter λ with various the material power law index n for $L/h = 20$

material of the beam can be assumed as metal and therefore the $\lambda_{cr} - n$ curve has an asymptote approximately after $n = 40$. In the case of $n = 0$, the functionally graded material beam is reduced to the homogeneous ceramics beam.

In Figs. 8, 9 and 10, dimensionless central deflections, dimensionless total axial extensions and dimensionless end constraint moments are shown for various dimensionless thermal load λ, material power law index n for $L/h = 20$ and $T_r = 3$. It is seen from Fig. 8 that the dimensionless central displacements and absolute value of the dimensionless end constraint moment increase considerably within the very small dimensionless thermal load increase after the critical thermal load is reached.

It is seen from Figs. 8, 9 and 10 that increase in the material power law index n causes increase in the dimensionless central deflections, dimensionless total axial extensions and absolute values of dimensionless end constraint moments respectively for all values of dimensionless thermal load λ for $L/h = 20$, $T_r = 3$: Because when the material power law index n increase, the material of the beam get close to the Aluminum and it is known from the physical properties of the Aluminum and
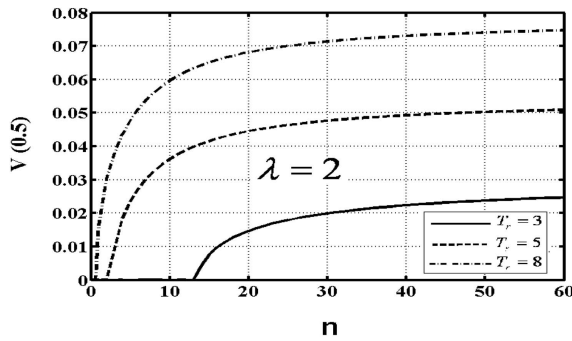
Fig. 11 The dimensionless specified deflections $V(0.5)$ versus the material power law index n for dimensionless thermal load parameter $\lambda = 2$ for $L/h = 20$
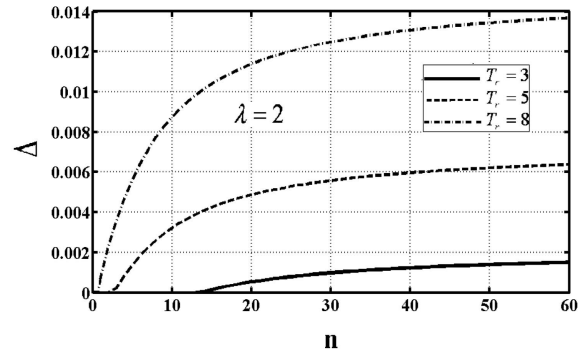

Fig. 12 The total axial extension Δ versus the material power law index n for dimensionless thermal load parameter $\lambda = 2$ for $L/h = 20$
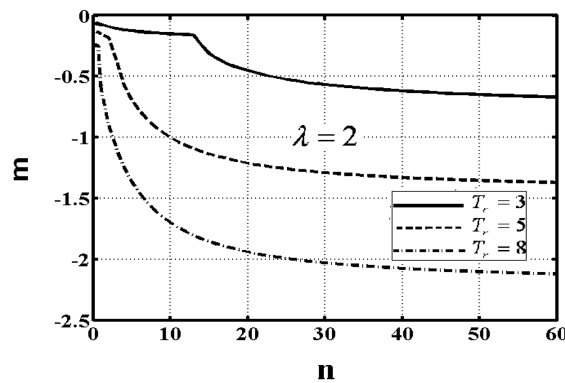

Fig. 13 The dimensionless end constraint moment m versus the material power law index n for dimensionless thermal load parameter $\lambda = 2$ for $L/h = 20$

Ceramics that the Young modulus of Ceramics is approximately two times greater than that of Aluminum.

It is seen from Figs. 11, 12 and 13 that increase in the ratio of temperature rise of top and bottom surfaces T_r of the beam causes increase in the dimensionless central deflections, dimensionless total axial extensions and absolute values of dimensionless end constraint moments respectively for all values of the material power law index n for $\lambda = 2$, $L/h = 20$: Because increase in the T_r causes increase in the bending moment distribution in the beam.

It is known that, in the failure analysis, the most important quantities are the principal Cauchy normal stresses $\sigma_{\max}, \sigma_{\min}$ which can be expressed as follows

$$\overline{\sigma}_{\max} = \frac{\overline{\sigma}_{xx} + \overline{\sigma}_{yy}}{2} + \sqrt{\left(\frac{\overline{\sigma}_{xx} - \overline{\sigma}_{yy}}{2}\right)^2 + (\overline{\sigma}_{xy})^2} \qquad (22)$$

$$\overline{\sigma}_{\min} = \frac{\overline{\sigma}_{xx} + \overline{\sigma}_{yy}}{2} - \sqrt{\left(\frac{\overline{\sigma}_{xx} - \overline{\sigma}_{yy}}{2}\right)^2 + (\overline{\sigma}_{xy})^2} \qquad (23)$$

Fig. 14 The dimensionless Cauchy maximum principal normal stresses versus dimensionless thermal load parameter λ for various material power law index n for $L/h = 20$ at central section ($\xi = 0.5$), $\eta = 0.5$
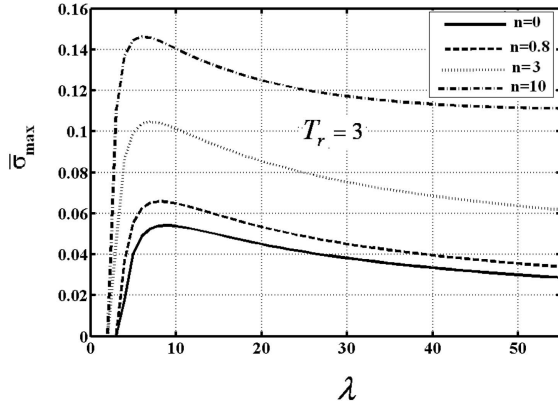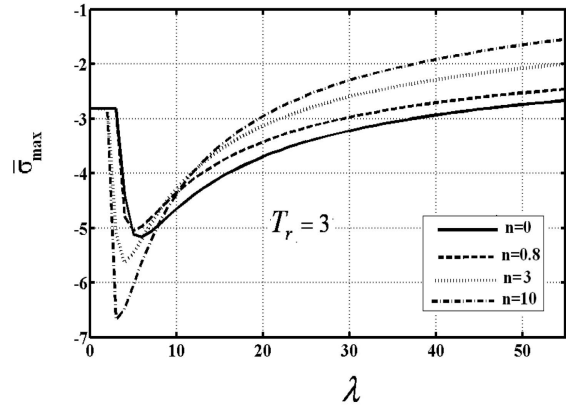

Fig. 15 The dimensionless Cauchy minimum principal normal stresses versus dimensionless thermal load parameter λ for various material power law index n for $L/h = 20$ at central section ($\xi = 0.5$), $\eta = 0.5$

Fig. 16 Dimensionless Cauchy maximum principal normal stress distributions along the height of the beam for some given values of the power-law index n at central section, $\xi = 0.5$, for $L/h = 20$, $\lambda = 4$ and $T_r = 3$
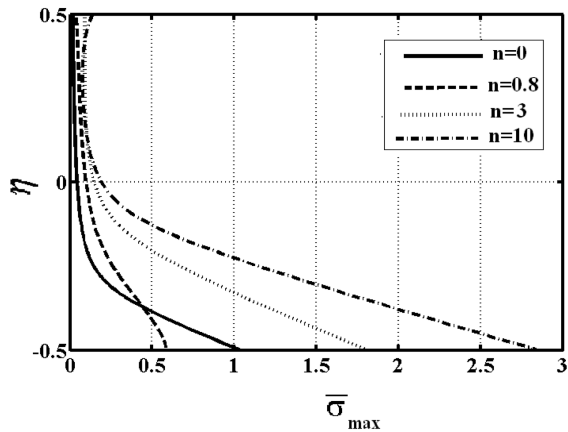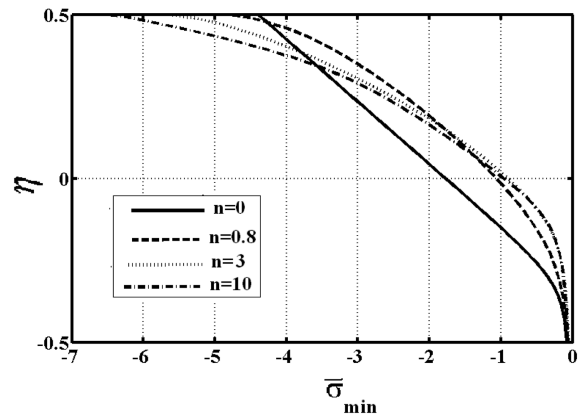

Fig. 17 Dimensionless Cauchy minimum principal normal stress distributions along the height of the beam for some given values of the power-law index n at central section, $\xi = 0.5$, for $L/h = 20$, $\lambda = 4$ and $T_r = 3$

It is seen from Fig. 14 and 15 that the dimensionless Cauchy maximum principal normal stresses and absolute value of dimensionless Cauchy minimum principal normal stresses at the point $\xi = 0.5$, $\eta = 0.5$ increase considerably within the very small dimensionless thermal load increase after the critical thermal load is reached. After the very small dimensionless thermal load increase after the critical load, the dimensionless maximum principal normal stresses and absolute value of dimensionless minimum principal normal stresses decrease monotonously. Also, for the same thermal loading, dimensionless maximum principal normal stresses and absolute value of dimensionless minimum stresses increase considerably when the material power law index n increases.

Dimensionless Cauchy maximum and minimum principal normal stress distributions along the height of the beam for some given values of the power-law index n at central section, $\xi = 0.5$, for $L/h = 20$, $\lambda = 4$ and $T_r = 3$ are given in the Figs. 16 and 17. It is seen from Figs. 16 and 17 that the material power law index n plays an important role on the dimensionless stress distributions along the height of the beam.

4. Conclusions

Buckling and post-buckling analysis of a functionally graded Timoshenko beam subjected to thermal loading are investigated by using the total Lagrangian Timoshenko beam element approximation. Material properties of the beam change in the thickness direction according to a power-law function. The beam is clamped at both ends. The considered highly non-linear problem is solved by using incremental displacement-based finite element method in conjunction with Newton-Raphson iteration method and the thermal buckling and post-buckling response of a transversally non-uniformly heated Timoshenko beam with clamped-clamped ends are obtained. The obtained results are in a very good harmony with the related available results in the literature.

The following conclusions are reached from the obtained results:

(1) Increase in the material power law index n causes increase in the dimensionless central deflections, dimensionless total axial extensions and absolute values of dimensionless end constraint moments respectively for all values of dimensionless thermal load λ for $L/h = 20$, $T_r = 3$.

(2) Increase in the ratio of temperature rise of top and bottom surfaces T_r of the beam causes increase in the dimensionless central deflections, dimensionless total axial extensions and absolute values of dimensionless end constraint moments respectively for all values of the material power law index n for $\lambda = 2$, $L/h = 20$.

3) The dimensionless maximum principal normal stresses and absolute value of dimensionless minimum principal normal stresses at the point $\xi = 0.5$, $\eta = 0.5$ increase considerably within the very small dimensionless thermal load increase after the critical thermal load is reached. After the very small dimensionless thermal load increase after the critical load, the dimensionless maximum principal normal stresses and absolute value of dimensionless minimum principal normal stresses decrease monotonously. Also, for the same thermal loading, dimensionless maximum principal normal stresses and absolute value of dimensionless minimum stresses increase considerably when the material power law index n increases.

4) The material power law index n plays an important role on the dimensionless stress distributions along the height of the beam.

References

Akbaş, Ş.D. and Kocatürk, T. (2011), "Post-buckling analysis of a simply supported beam under uniform thermal loading", *Sci. Res. Essay.*, **6**(4), 1135-1142.

Akbaş, Ş.D. (2011), "Thermal post-buckling analysis of functionally graded beams", PhD Thesis Term Report on May and November, Institute of Science at Yildiz Technical University (İstanbul).

Akbaş, Ş.D. and Kocatürk, T. (2011), "Eksenel Doğrultuda Fonksiyonel derecelendirilmiş Timoshenko kirişinin sıcaklık etkisi altındaki burkulma sonrası davranışının incelenmesi (Post-buckling behavior of axially functionally graded Timoshenko beam under the influence of temperature)", *XVII. Turkish National Mechanic*

Congress, Elazığ, Turkey, In Print (in Turkish).

Alibeigloo, A. (2010), "Thermoelasticity analysis of functionally graded beam with integrated surface piezoelectric layers", *Compos. Struct.*, **92**, 1535-1543.

Anandrao, K.S., Gupta, R.K., Ramchandran, P. and Rao, V. (2010), "Thermal post-buckling analysis of uniform slender functionally graded material beams", *Struct. Eng. Mech.*, **36**(5), 545-560.

Bhangale, R.K. and Ganesan, N. (2006), "Thermoelastic buckling and vibration behavior of a functionally graded sandwich beam with constrained viscoelastic core", *J. Sound Vib.*, **295**, 294-316.

Carpinteri, A. and Paggi, M. (2008), "Thermo-elastic mismatch in nonhomogeneous beams", *J. Eng. Mat.*, **61**(2-4), 371-384.

Ching, H.K. and Yen, S.C. (2005), "Meshless local Petrov-Galerkin analysis for 2D functionally graded elastic solids under mechanical and thermal loads", *Composites: Part B*, **36**, 223-240.

Ching, H.K. and Yen, S.C. (2005), "Transient thermoelastic deformations of 2-D functionally graded beams under nonuniformly convective heat supply", *Compos. Struct.*, **73**, 381-393.

Farid, M., Zahedinejad, P. and Malekzadeh, P. (2010), "Three-dimensional temperature dependent free vibration analysis of functionally graded material curved panels resting on two-parameter elastic foundation using a hybrid semi-analytic, differential quadrature method", *Struct. Eng. Mech.*, **31**(1), 2-13.

Felippa, C.A., Retrieved May (2011), "Notes on nonlinear finite element methods", http://www.colorado.edu/engineering/cas/courses.d/NFEM.d/NFEM.Ch09.d/NFEM.Ch09.pdf

Inan, O., Dag, S. and Erdogan, F. (2005), "Three dimensional fracture analysis of FGM coatings", *Mater. Sci. Forum*, **492-493**, 373-378.

Kapuria, S., Bhattacharyya, M. and Kumar, A.N. (2008), "Theoretical modeling and experimental validation of thermal response of metal-ceramic functionally graded beams", *J. Therm. Stresses*, **31**, 759-787.

Ke, L.L., Yang, J. and Kitipornchai, S. (2009), "Postbuckling analysis of edge cracked functionally graded Timoshenko beams under end shortening", *Compos. Struct.*, **90**(2), 152-160.

Khdeir, A.A. (2001), "Thermal buclding of cross-ply laminated composite beams", *Acta Mechanica*, **149**, 201-213.

Kiani, Y. and Eslami, M.R. (2010), "Thermal buckling analysis of functionally graded material beams, *Int. J. Mech. Mater. Des.*, **6**(3), 229-238.

Kocatürk, T., Şimşek M. and Akbaş, Ş.D. (2011), "Large displacement static analysis of a cantilever Timoshenko beam composed of functionally graded material", *Sci. Eng. Compos. Mater.*, **18**, 21-34.

Kocatürk, T. and Akbaş, Ş.D. (2011), "Post-buckling analysis of Timoshenko beams with various boundary conditions under non-uniform thermal loading", *Struct. Eng. Mech.*, **40**(3), 347-371.

Librescua, L., Oha, S.Y. and Songb, O. (2005), "Thin-walled beams made of functionally graded materials and operating in a high temperature environment: vibration and stability", *J. Therm. Stresses*, **28**, 649-712.

Li, S.R., Zhang, J.H. and Zhao, Y.G. (2006), "Thermal Post-Buckling of functionally graded material Timoshenko beams", *Appl. Math. Mech.*, **26**(6), 803-810..

Li, S.R., Su, H.D. and Cheng, C.J. (2009), "Free vibration of functionally graded material beams with surface-bonded piezoelectric layers in thermal environment", *Appl. Math. Mech.*, **30**(8), 969-982.

Lim, C.W., Yang, Q. and Lu, C.F. (2009), "Two-dimensional elasticity solutions for temperature dependent in-plane vibration of FGM circular arches", *Compos. Struct.*, **90**, 323-329.

Lu, C., Chen, W. and Zhong, Z. (2006), Two-dimensional thermoelasticity solution for functionally graded thick beams", *Science in China Series G: Physics, Mechanics & Astronomy* **49**(4), 451-460.

Malekzadeh, P., Haghighi, M.R.G. and Atashi, M.M. (2010), "Out-of-plane free vibration of functionally graded circular curved beams in thermal environment", *Compos. Struct.* **92**(2), 541-552.

Mohammadia, M. and Drydena, J.R. (2008), "Thermal stress in a nonhomogeneous curved beam", *J. Therm. Stresses*, **31**(7), 587-598.

Na, K.S. and Kim, J.H. (2006), "Thermal postbuckling investigations of functionally graded plates using 3-D finite element method", *Finite Elem. Analy. Des.*, **42**(8-9), 749-756.

Nirmula, K., Upadhyay, P.C., Prucz, J. and Lyons, D. (2006), "Thermo-elastic Stresses in Composite Beams with Functionally Graded Layer", *J. Reinf. Plast. Compos.*, **25**(12), 1241-1254.

Pradhan, S.C. and Murmu, T. (2009), "Thermo-mechanical vibration of FGM sandwich beam under variable elastic foundations using differential quadrature method", *J. Sound Vib.*, **321**, 342-362.

Rahimi, G.H. and Davoodinik, A.R. (2008), "Thermal behavior analysis of the functionally graded Timoshenko's beam", *IUST Int. J. Eng. Sci.,* **19**(5-1), 105-113.

Rastgo, A., Shafie, H. and Allahverdizadeh, A. (2005), "Instability of curved beams made of functionally graded material under thermal loading, International", *J. Mech. Mater. Des.,* **2**, 117-128.

Reddy, J.N. (2004), *An Introduction to Non-linear Finite Element Analysis*, Oxford University Press Inc., New York.

Sankar, B.V. and Tzeng, J.T. (2002), "Thermal stresses in functionally graded beams", *AIAA J.*, **40**(6), 1228-1232.

Song, X. and Li, S. (2008), "Nonlinear stability of fixed-fixed FGM arches subjected to mechanical and thermal load", *Adv. Mater. Res.,* **33-37**, 699-706.

Xiang, H.J. and Yang, J. (2008), "Free and forced vibration of a laminated FGM Timoshenko beam of variable thickness under heat conduction", *Composites: Part B,* **39**, 292-303.

Wakashima, K., Hirano, T. and Niino, M. (1990), "Space applications of advanced structural materials", *ESA,* SP: 303-397.

Zienkiewichz, O.C. and Taylor, R.L. (2000), *The Finite Element Method*, Fifth Edition, Volume 2, Solid Mechanics, Butterworth-Heinemann, Oxford.